Different structural states in oligonucleosomes are required for early versus late steps of base excision repair

Shima Nakanishi[1], Rajendra Prasad[2], Samuel H. Wilson[2] and Michael Smerdon[1],*

[1]Biochemistry and Biophysics, School of Molecular Biosciences, Washington State University, Pullman, WA 99164-4660 and [2]National Institute of Environmental Health Sciences, P.O. Box 12233, Research Triangle Park, NC 27709-2233, USA

ABSTRACT

Chromatin in eukaryotic cells is folded into higher order structures of folded nucleosome filaments, and DNA damage occurs at all levels of this structural hierarchy. However, little is known about the impact of higher order folding on DNA repair enzymes. We examined the catalytic activities of purified human base excision repair (BER) enzymes on uracil-containing oligonucleosome arrays, which are folded primarily into 30 nm structures when incubated in repair reaction buffers. The catalytic activities of uracil DNA glycosylase (UDG) and apyrimidinic/apurinic endonuclease (APE) digest G:U mismatches to completion in the folded oligonucleosomes without requiring significant disruption. In contrast, DNA polymerase β (Pol β) synthesis is inhibited in a major fraction (∼80%) of the oligonucleosome array, suggesting that single strand nicks in linker DNA are far more accessible to Pol β in highly folded oligonucleosomes. Importantly, this barrier in folded oligonucleosomes is removed by purified chromatin remodeling complexes. Both ISW1 and ISW2 from yeast significantly enhance Pol β accessibility to the refractory nicked sites in oligonucleosomes. These results indicate that the initial steps of BER (UDG and APE) act efficiently on highly folded oligonucleosome arrays, and chromatin remodeling may be required for the latter steps of BER in intact chromatin.

INTRODUCTION

DNA is a constant target of spontaneous hydrolysis at 37°C (1). Two frequent hydrolysis reactions are depurination to produce non-coding abasic (AP) sites, and deamination of cytosine to generate uracil (U) (2,3). Minor base lesions and single-strand breaks are repaired primarily by base excision repair (BER) in mammalian cells. The first step of BER is removal of the damaged base by a DNA glycosylase, cleaving the *N*-glycosyl bond between the base and deoxyribose (4,5). This results in forming apurinic or apyrimidic (AP) sites in DNA. As noted earlier, AP sites can also occur from depurination or depyrimidination yielding a common intermediate in BER. Subsequently, AP-endonuclease 1 (APE) incises the damaged strand 5′ to the AP-site generating a 3′-hydroxyl and a 5′ deoxyribose phosphate (dRP) (6). Then, short-patch BER proceeds by action of DNA polymerase β (Pol β), filling the single-nucleotide gap and removing the dRP group (7). Finally, the nick is sealed by DNA ligase I or III. Generally, replication and transcription are not significantly stalled at these types of base lesions. As a result, they can be mutagenic if not repaired (8) resulting in genomic instability and such chronic disorders as cancer.

BER enzymes must deal with damage generated throughout the genome, and the majority of eukaryotic DNA is packaged into highly condensed structures (9). As shown in previous studies *in vitro* using mononucleosomes (10,11), BER enzymes are significantly suppressed in mononucleosomes. However, recently, considerable flexibility of mononucleosome DNA has been reported (12,13), particularly at the sites of entry and exit from the nucleosome. Such dynamic properties of nucleosomes may allow certain small proteins to gain access to DNA. For example, it was found that Dnmt3a and Dnmt1 DNA methyltransferases act more efficiently on nucleosome DNA than naked DNA, and do not require disruption of histone octamers (14). Furthermore, Thoma and colleagues (15) have shown that UV photolyase, a light-dependent DNA repair enzyme, recognizes and repairs

---

CPDs in nucleosomes within seconds in intact yeast cells, suggesting this protein takes advantage of nucleosome dynamics to gain access to CPDs in chromatin.

Although dynamic properties of nucleosomes may contribute to the accessibility of DNA, they are not sufficient for some bulky proteins or protein complexes to gain access to internal sites. Indeed, several different types of chromatin remodeling factors have been identified that assist DNA accessibility. One class of these factors changes histone-DNA contacts by adding or removing covalent modifications from histone tails. Another class alters chromatin structure in a non-covalent manner using ATP hydrolysis, and this class has been subdivided into different families based on the ATPase subunit (16). The effect of ATP-dependent chromatin remodeling on overall DNA repair has been shown using mono- or di-nucleosomes (17–19). Recently, we reported that the SWI/SNF remodeling complex facilitates nucleotide excision repair (NER) of UV damage in yeast cells (20). However, the question of whether chromatin remodeling is required prior to damage recognition or during DNA repair has not been addressed. Furthermore, the initiation of DNA repair in highly compact chromatin remains an essential component for the understanding of BER in cells. Most BER enzymes are essential (21,22), making it more difficult to assess this pathway *in vivo*. However, a complete understanding of DNA repair *in vivo* will remain elusive until the impact of higher order chromatin folding on repair enzymes is understood. Therefore, we are establishing conditions *in vitro* that more closely resemble physiologic templates *in vivo* to study BER in chromatin.

In this work, the process of short-patch BER was studied *in vitro* using purified human BER enzymes and highly folded oligonucleosomes containing DNA with uracil at different sites. We measured the efficiency of uracil removal by UDG and APE from G:U mismatch base pairs in oligonucleosomes reconstituted with 12 tandem repeats of a 208 bp segment (208–12) of *Lytechinus variegates* 5S rDNA. In addition, we examined the effect of yeast chromatin remodeling complexes ISW1 and ISW2 on Pol β DNA synthesis in these oligonucleosome arrays. To our knowledge, this is the first study examining DNA repair at the 30 nm oligonucleosome fiber level of DNA packaging in chromatin and linking chromatin remodeling with BER.

MATERIALS AND METHODS

Preparation of uracil-containing template DNA

Linearized plasmid pSL208-12 was denatured in freshly prepared NaOH (0.32 M) and mixed with 2× volume of 2% low melting agarose. Before it solidified, the mixture was transferred to mineral oil to form a bead. Each bead contained ∼500 ng/μl of DNA. A 5 M sodium bisulfite solution was mixed with 0.2 volume hydroquinone solution, and the pH adjusted to 5.0. Freshly prepared sodium bisulfite solution was added gently to the tube containing a bead. The tube was covered with foil and incubated at room temparature for 15 min.

Following chemical treatment, the bead was washed 10 times with 1 ml TE buffer. Desulfonation was carried out by suspension in 0.2 M NaOH for 10 min, followed by extensive washing in TE buffer overnight. DNA was then extracted from the agarose beads, annealed, and digested with restriction enzymes to generate 208-12 templates for further use. The reaction was optimized such that the majority of single-strand DNA fragments received 1–2 uracils.

Reconstitution of nucleosomal arrays—Histone octamers were prepared from chicken erythrocyte nuclei as described (23). Oligonucleosome arrays were reconstituted from histone octamers and purified 208-12 DNA template using salt dialysis methods (24,25). The degree of template saturation was controlled by varying the ratio of moles histone octamer to moles 208-bp DNA from 0.9 to 1.2. In our system, a ratio of 1.1 provided optimal efficiency of reconstitution.

EcoRI digestion assay

An aliquot of 700 ng of oligonucleosomes (or naked DNA) was digested with EcoRI restriction enzyme in a buffer containing 10 mM Tris, pH 8.0, 125 mM NaCl, 2.5 mM $MgCl_2$ and 1 mM EDTA for 2 h at 37°C. The reaction was stopped by adding gel loading buffer, containing SDS, and the samples run in 5% polyacrylamide gels in 1× TBE.

Analytical Ultracentrifugation

Sedimentation velocity experiments were performed in a Beckman XL-A analytical ultracentrifuge utilizing scanner optics at 260 nm. The temperature was equilibrated at 20°C under vacuum for at least 1h prior to the run and was controlled during the run to within ±0.1°C. Scans were analyzed by the method of van Holde and Weischet (26) using UltraScan 7.4 (B. Demeler, San Antonio, TX, USA).

UDG/APE digestion

The UDG and APE reaction mixture contained 50 mM Hepes, pH 7.5, 2 mM DTT, 0.2 mM EDTA, pH 8.0, 100 μg/ml BSA, 10% glycerol (wt/vol) and 2.5 mM $MgCl_2$. A lower Mg^{2+} concentration was used than in previous studies to prevent oligonucleosomes from aggregating. Reactions were initiated by adding UDG and APE (1 nM or 10 nM final concentration), and incubations were carried out at 37°C for 0 to 1h. Aliquots were removed at different times and treated with phenol to stop the reaction. Digested DNA was resolved on denaturing alkaline gels, transferred to a Hybond-N+ membrane (GE Healthcare, England), probed with randomly labeled 5S rDNA fragments, and visualized on a PhosphorImager (model 445-P90, Molecular Dynamics). Images were analyzed with IMAGE QUANT software (Molecular Dynamics).

High-resolution mapping of UDG/APE cleavage sites in 208-12 nucleosomal arrays

To uniformly enhance the signal of each fragment after UDG/APE digestion, the resulting ss-fragments (up to 2.5 kb) were annealed with biotin-labeled primers and purified using streptavidin magnetic beads, as previously described (27). Briefly, biotin-attached oligonucleotides, containing a sequence complementary to the 3′-end of 208-12 DNA ([biotin]NNNNNNTTTTTGCATGCCTG CAGGTC), were synthesized and the biotin group was used to separate annealed fragments from the rest. The 6 Ns ensured full-length labeling of the fragment, and the 5 Ts allowed the annealed fragment to be extended with [α-^{32}P]dATP. Labeled fragments were separated in a 5.5% polyacrylamide denaturing gels.

Pol β DNA synthesis

DNA synthesis with Pol β was performed in a mixture containing 50 mM Hepes, pH 7.5, 2 mM DTT, 0.2 mM EDTA, 100 μg/ml BSA, 10% glycerol (wt/vol), 4 mM ATP, 5 mM MgCl$_2$ and [α-^{32}P]dCTP. Templates were first incubated with UDG and APE (10 nM each) for 10 min. DNA synthesis was then initiated by addition of Pol β and incubations were at 37°C for 0–4 h. Aliquots were removed at different times and treated with phenol to stop the reaction. Samples were then run on a native agarose gels and the gels stained with ethidium bromide. Gels were then blotted onto membrane, visualized on a Phosphorimager and the images analyzed with IMAGE QUANT software.

Effect of yISW1 and yISW2 activity on Pol β DNA synthesis

Pol β DNA synthesis reactions were carried out with oligonucleosomes under identical conditions as above, with or without chromatin remodeling complex. Remodeling complexes, yISW1 or yISW2 (generous gift of Dr Tsukiyama) were added at the beginning of repair synthesis. The molar ratio of ISW1 or ISW2 to mononucleosomes was 1.

RESULTS

Nucleosome arrays containing G:U mismatches can form higher order structures. The experiments described in this report utilize a DNA fragment composed of 12 tandem repeats of a 208 bp segment of the *L. variegates* 5S rRNA gene as a template for reconstitution of oligonucleosomes (Figure 1A). Each repeat contains sequences that position nucleosomes both translationally and rotationally on the DNA molecule (28). To study short-patch BER, uracil was incorporated at cytosine bases in the 208-12 DNA fragment by treatment with sodium bisulfite. This reaction was optimized to yield a majority of the single-stranded (ss) fragments with 1 or 2 uracils. For example, 35% of the fragments used for UDG/APE digestion (1 nM each) contained a single uracil, 23% contained two uracils, and 15% of the fragments contained more than two uracils.

DNA-stripped histone octamers from chicken erythrocytes were reconstituted by stepwise salt dialysis (24,25)
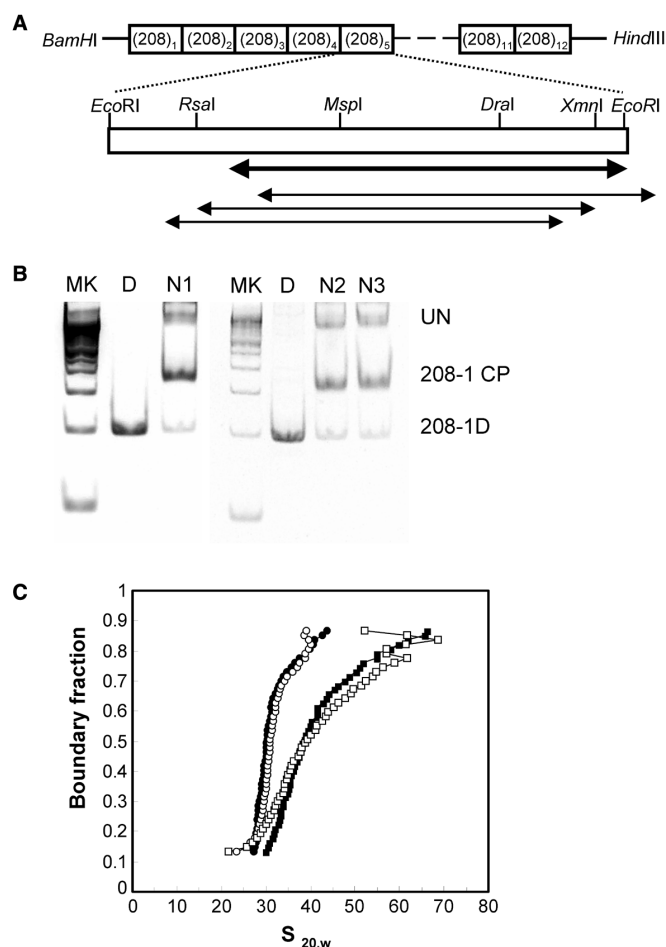
Figure 1. Reconstitution of oligonucleosomes containing G:U mismatches. (**A**) Schematic of 208-12 template. Templates used in this work were composed of 12 tandem repeats of a 208 bp 5S rRNA gene sequence. Thick arrow indicates the major nucleosome position, and thin arrows indicate the minor nucleosome positions. (**B**) Degree of nucleosome loading. Oligonucleosomes containing either control DNA (N1) or DNA with uracils (N2 and N3) were digested with *EcoR*I, electrophoresed in native 5% polyacrylamide gels and stained with ethidium bromide. MK denotes 100 bp DNA ladder; and UN, 208-1 CP and 208-1 D, denote undigested nucleosomal arrays, mononucleosomes and naked DNA, respectively. (**C**) Sedimentation velocity analysis of nucleosome arrays with and without uracil. Samples in either TE buffer or TE with 2 mM MgCl$_2$ were equilibrated at 20°C and sedimented at either 18 000 or 20 000 rpm. Shown are the sedimentation coefficient distribution plots for nucleosome arrays with (open symbols) or without (closed symbols) uracil residues in TE buffer (circles) and TE buffer + 2 mM MgCl$_2$ (squares).

onto a non-damaged 208-12 template or a 208-12 template containing G:U mismatches. Initially, varying ratios (r) of histone octamers to 5S rDNA repeats were used for reconstitution to generate a fully loaded oligonucleosome array. To evaluate the degree of nucleosome loading, two different methods were used. First, gel mobility shift assays, following restriction digestion with EcoRI, were used. Since each repeat is flanked by EcoRI sites (Figure 1A), a mononucleosome or 208-1 free DNA is released after EcoRI digestion. When only about 2–5% of the 5S repeats are released in the free form, the 208-12 rDNA is considered to be fully saturated with

nucleosomes (29). We obtained fully saturated oligonu- cleosomes when r = 1.1 (25). Importantly, no significant differences in efficiency of oligonucleosome assembly were detected between intact 208-12 oligonucleosomes and those containing uracil (Figure 1B). This result was expected since the G:U-mismatch has the capacity to form base pairs (30). In addition, no additional disruption of the core particles was observed in the reconstituted oligonucleosomes in the BER reaction mixture buffer employed in this study (Figure 1B).

Sedimentation velocity analysis was also carried out to monitor the homogeneity of reconstituted oligonucleo- some arrays, as well as the degree of salt-induced higher order structure formation. The majority of nucleosomal arrays both with and without uracil residues sediment as rather homogeneous populations of 28–30S species in low ionic strength buffer (Figure 1C). The small fraction of material with larger S values was due to super-saturated nucleosome arrays assembled with additional histones. Furthermore, as the BER buffer used in this study contains Mg^{2+}, the Mg^{2+}-dependent folding of 208-12 oligonucleosomes was characterized. Hansen and col- leagues have shown that saturated 208-12 nucleosome arrays form a maximally folded 55S structure in 1–2 mM $MgCl_2$, with an extent of compaction equivalent to the classical higher order 30 nm structures (31). In the presence of 2 mM Mg^{2+}, S values of both intact oligonucleosomes (open symbols) and uracil-containing oligonucleosomes (closed symbols) were shifted to higher values (more compact structures) in a similar manner (Figure 1C). These results suggest that intramolecular folding of uracil-containing oligonucleosomes in solution is not disrupted in any significant way by G:U mismatches.

UDG and APE recognize and act on base lesions in folded oligonucleosomes. Incubation of either uracil- containing naked 208-12 DNA or oligonucleosomes with UDG and APE generates a single strand break that can be visualized on denaturing agarose gels (Figure 2). When digested with 1 nM each of UDG and APE, shorter bands are generated and the intensity of full-length (undigested) fragments is reduced during increasing digestion times (Figure 2A). Furthermore, the disappearance of full- length fragments is slower with oligonucleosomes than with naked 208-12 DNA (Figure 2A, graph), suggesting that the combined activity of these enzymes is reduced when DNA is folded into nucleosome arrays. The calculated initial rates for these digestion curves indicate that nucleosome arrays are digested ~2–3-fold slower by the combined action of UDG and APE. At higher enzyme concentrations (10 nM each), however, the digestion reaction proceeded to near-completion with folded oligo- nucleosomes (Figure 2B). This result indicates that these enzymes can access G:U sites within higher order structures of chromatin and do not require a marked disruption of DNA-histone contacts.
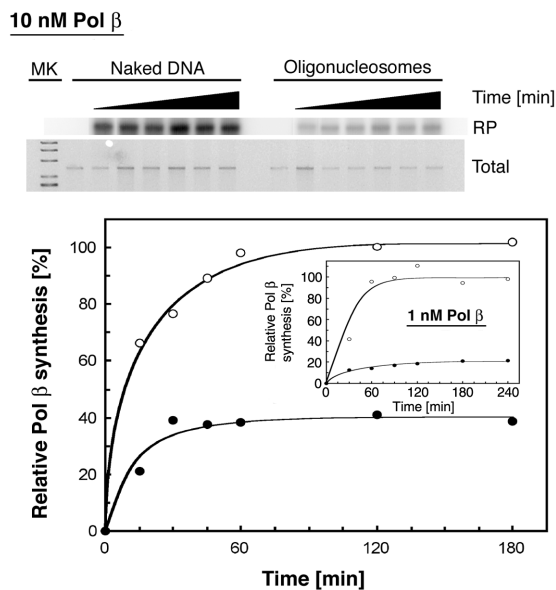
High resolution mapping of UDG/APE cleavage sites at uracils can be observed on DNA sequencing gels (Figure 2C). Overall, incision at damaged sites within linker DNA regions (between ovals) was faster than in core DNA (within ovals). However, a few sites within each of the nucleosome core particles were cleaved considerably faster than others (Figure 2C, red arrows). The rate of cleavage at these sites may reflect (i) the influence of flanking sequences in each of the 5S rDNA repeats, as observed for other DNA sequences (32), and/or (ii) the location of these sites at more accessible locations in the nucleosome cores (e.g. facing away from the histone surface in each nucleosome). In addition, some incised sites are detected within each of the repeats in the absence of UDG/APE digestion (Figure 2C, dotted arrows on left of 0 min lane), indicating that some fragments contained nicks at specific sites following the sodium bisulfite treatment. Although DNA was treated for short times with high concentrations of bisulfite to limit these nicks, the glycosyl bond at purine residues is still susceptible to hydrolysis under acidic conditions. The resulting AP sites lead to single strand breaks during desulfonation under alkaline conditions. However, because these nicked sites do not change during the UDG/APE digestion, they serve as an intrinsic control for the enzyme-produced sites (Figure 2C, dotted arrows).

Gap-filling by DNA Pol β is inhibited by oligonucleo- some formation. To assess activity of Pol β, the single- nucleotide repair patch was labeled with [α-^{32}P]dCTP. At a concentration of 1 nM, Pol β efficiently incorporates dCMP into naked DNA and reaches a plateau after 90 min (Figure 3 inset, open circles). On the other hand, at this concentration, Pol β only incorporates dCMP into ~20% of the sites in oligonucleosomes (Figure 3 inset, closed circles). The oligonucleosome template used in this study includes about 60 bp of linker DNA between nucleosome core particles (i.e. ~30% of the total DNA). Therefore, folded nucleosomes may affect the efficiency of DNA synthesis in the linker DNA region. Indeed, even at a 10-fold higher concentration of Pol β (10 nM), DNA synthesis on oligonucleosomes proceeded to a plateau of 37% in ~60 min (Figure 3), indicating that nucleosome core particles are a formidable barrier for the efficient addition of nucleotides by Pol β in oligonucleosomes. Therefore, it is possible that other factor(s) assist this step in intact cells.

Chromatin remodeling complex ISWI facilitates DNA synthesis by Pol β in oligonucleosomes. To investigate whether ATP-dependent chromatin remodeling facilitates Pol β DNA synthesis, purified yeast remodeling complexes ISW1 and ISW2 (33) were tested with our BER-oligonucleosome model system. ISWI complexes induce nucleosome sliding both *in vivo* and *in vitro* (34), which makes DNA segments accessible while maintaining the overall packaging of DNA (35). The ISWI complex is present in all eukaryotes, with the exception of *Schizosaccharomyces pombe* (36), and is relatively abun- dant. For example, ISWI is expressed during *Drosophila* development at levels as high as 100 000 molecules/cell (37). Moreover, ISWI induces nucleosome sliding on nicked DNA (35), which makes the ISWI remodeling complex a good candidate for assisting the Pol β step of the BER pathway in cells. A quantitative comparison of the synthesis of Pol β on oligonucleosomes in the absence and presence of these complexes was made by setting the maximum DNA synthesis achieved on oligonucleosomes in the absence of these factors to 1. As shown in Figure 4,

Figure 2. UDG and APE digestion of dU-containing oligonucleosomes. (**A**) Alkaline agarose gels of naked 208-12 DNA and oligonucleosomes after incubation with 1 nM each of UDG and APE. Time course is from 0 to 1 h, and MK denotes 100 bp and 1 kb DNA ladders. Plot shows % DNA incised by 1nM UDG and APE for naked DNA (open circle) and oligonucleosomes (filled circle) following different digestion times. (**B**) Same as in (A), except 10 nM each of UDG and APE were used. (**C**) High resolution mapping of UDG/APE cleavage sites. Oligonucleosomes digested with UDG/APE for 0, 1, 5, 15 and 60 min (Lane 1–5, respectively) were end-labeled as described in Materials and Methods section, and were electrophoresed in denaturing gels for 6 h (left panel) and 12 h (right panel). Nucleosome positions are indicated by ovals where numbers denote nucleosome position from end of the fragment. Rapidly cleaved sites within a nucleosome core are indicated by red arrows. Initially nicked sites before UDG/APE digestion are indicated by dotted arrows, which serve as controls.

both of the yeast ISWI complexes promote efficient dCMP incorporation at cleaved uracil sites in the oligonucleosome templates. Indeed, after 4 h, ISW1 and ISW2 increased incorporation by ∼4-fold and ∼6-fold, respectively. Thus, both remodeling complexes significantly increase the accessibility of nucleosome DNA to Pol β.

DISCUSSION

In facing the steric hurdles to surveying the genome, DNA repair proteins may take advantage of the dynamic properties of chromatin and/or rely on other factors to remodel local regions of DNA damage. It has been shown that nucleosome structure reduces the accessibility of many different types of DNA processing proteins, and chromatin remodellers such as SWI/SNF enable the access by these proteins (16,38). In the case of DNA repair, the question arises as to whether cells require chromatin remodeling prior to or during the repair process. Here, we show that two different chromatin states may be required for efficient BER by systematically examining BER *in vitro*, using highly folded nucleosome arrays of the 208-12 5S rDNA sequence, that more closely resemble natural substrates in intact cells than mono- (or di-) nucleosomes.

Uracil-containing DNA does not inhibit nucleosome formation or compaction. In this study, chemical deamination of cytosine to uracil was carried out to generate 1–2

10 nM Pol β

Figure 3. Pol β synthesis in dU-containing oligonucleosomes. After digestion of both naked DNA and oligonucleosome DNA with UDG and APE (10 nM each), samples were incubated with 10 nM Pol β for different times and electrophoresed on a native agarose gel. Upper gel, repair patch incorporation of [α-^{32}P]dCMP into 208-12 DNA (RP). Lower gel, total DNA stained with ethidium bromide (total). Plot shows time course of [α-^{32}P]dCMP incorporation into naked DNA (open cicle) and oligonucleosomes (filled circle) by 10 nM Pol β. Incorporation values were normalized to naked DNA maximum, following 15, 30, 45, 60, 120 and 240 min incubation time. (inset) Time course of [α-^{32}P]dCMP incorporation into naked DNA (open circle) and oligonucleosomes (filled circle) by 1 nM Pol β.

uracils/ss-fragment (i.e. ~2–4 G:U mismatches in each array template). A G:U mismatch has the capacity to form a base pair (30), which is most likely why these lesions do not affect nucleosome formation or compaction (Figure 1). This aspect of non-distorting DNA lesions makes their recognition more difficult than that of helix distorting DNA lesions such as *cis-syn* cyclobutane pyrimidine dimers caused by UV light, which bend the long axis of DNA ~ 30° (39). Furthermore, our sedimentation velocity results demonstrate that the reconstituted nucleosome arrays containing G:U mismatches form higher-order structures at increased ionic strength. Finally, cytosine deamination occurs more frequently where a segment of ssDNA is temporary exposed during transcription and replication (1). Our data supports the notion that such uracil-containing DNA can reassemble into nucleosomes and fold back into more compact structures in intact cells, if not repaired.

UDG and APE can access DNA base damage even in highly folded regions of chromatin. Differences occur in the activities of UDG and APE at different sites of oligonucleosomes, depending on the predicted rotational settings of the lesions as well as the flanking sequences (Figure 2C), in agreement with previous studies on mononucleosomes (10,11). More importantly, however, these enzymes digest the highly folded arrays to completion in a concentration-dependent manner, indicating that both enzymes are capable of accessing dU-damaged sites
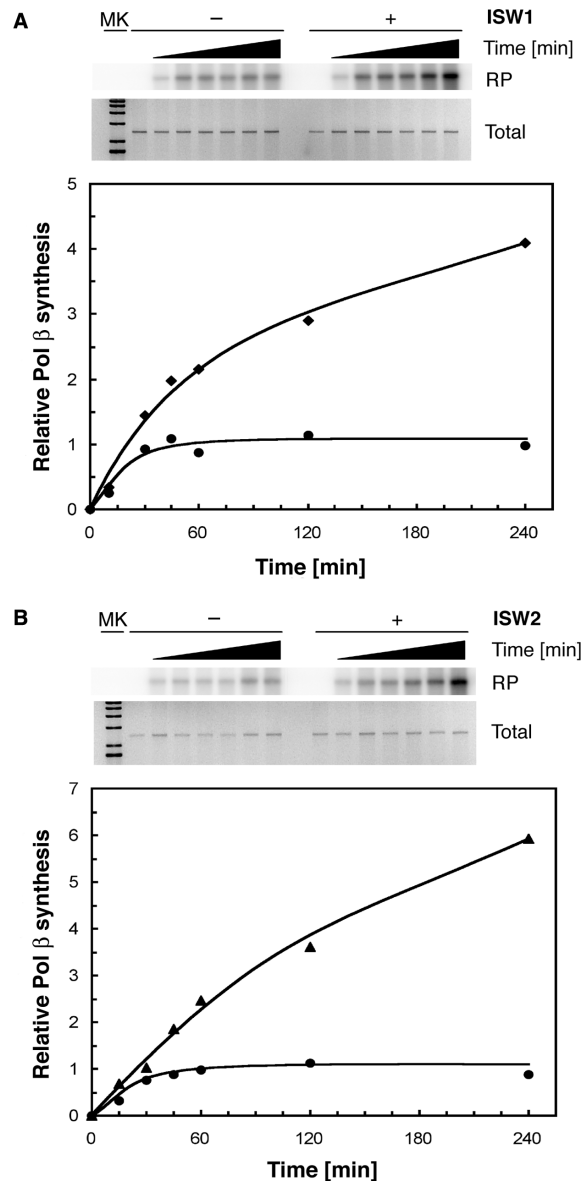
Figure 4. Effect of yISW1 and yISW2 on Pol β synthesis in dU-containing oligonucleosomes. (**A**) Native agarose gel showing Pol β DNA synthesis, following different incubation times in the absence (−) and presence (+) of ISW1. Upper gel, shows incorporation of [α-^{32}P]dCMP into 208-12 DNA (RP). Lower gel, total DNA stained with ethidium bromide (total). Plot shows time course of [α-^{32}P]dCMP incorporation by 1 nM Pol β in the presence (diamond) and absence (circles) of ISWI1, relative to maximum incorporation value for oligonucleosomes in the absence of ISW1. (**B**) Native agarose gels and time course plot showing Pol β DNA synthesis in the absence (−, filled circle) and presence (+, filled triangle) of ISW2.

within nucleosomes in a higher-order structure of chromatin (Figure 2). Moreover, the strong inhibition of Pol β activity by oligonucleosomes following digestion with high concentrations of UDG/APE (Figure 3) indicates there is no significant nucleosome disruption by UDG/APE digestion. Whether chromatin remodeling or recognition of DNA lesions would come first during BER in cells is unclear at this time. Phosphorylation of histone variant H2AX following induction of DNA double-strand breaks

(DSBs) by ionizing irradiation (40,41) is known to play an important role in recruiting DSB-recognition and repair proteins (42), chromatin remodeling factors (43) and DNA damage-induced checkpoint proteins (44). However, unlike induced DSBs, different types of minor base alterations occur constantly throughout the genome and, to date, there is no *in vivo* evidence showing that a specific histone modification is formed following DNA base damage. Our data suggests that, at least for BER, a variety of base lesions could be recognized directly by a substrate specific glycosylase in chromatin without requiring significant local chromatin remodeling. UDG and APE are relatively small, and bend the long axis of DNA only ∼20° and ∼35°, respectively, upon binding (45,46). Such bending may be compatible with the DNA flexibility allowed on the nucleosome surface. Furthermore, such 'direct recognition' by these enzymes may be critical for the cell to initiate BER in chromatin, especially in heterochromatin.

Pol β DNA synthesis requires local chromatin remodeling. Unlike the UDG and APE enzymes, Pol β is strictly inhibited by the folding of DNA into nucleosome arrays (Figure 3). In addition to our previous observation on mononucleosomes (11), our results clearly indicate that the major restriction of BER in oligonucleosome templates is the Pol β step. However, our new results indicate there are two levels of inhibition of Pol β in oligonucleosomes. At a lower concentration of Pol β (1 nM), ∼80% of the total gaps are not filled (Figure 3, inset) in oligonucleosome arrays, which is equivalent to the portion of potential uracil sites (i.e. dC sites) in 168 bp of nucleosomal DNA within the 208 bp repeat. However, when the concentration of Pol β is increased 10-fold, ∼63% of total gaps remain unfilled (Figure 3), which is almost equivalent to the fraction of potential uracil sites in the 147 bp nucleosome core DNA (65%). This indicates that the outer 10 bp of DNA at the points of entry and exit to the nucleosome are more accessible in oligonucleosomes than the inner 147 bp of core DNA.

Pol β binding requires an ∼90° bend in the DNA molecule (47), and such a radical distortion may not be tolerated by nucleosomes. This result may reflect the requirement for additional factor(s) to release the structural constraints of positioned nucleosomes in intact cells. Since BER intermediates such as single-strand breaks are also mutagenic, it is crucial that, once initiated, completion of BER occurs rapidly in cells. Therefore, we explored possible solutions for Pol β to overcome such structural barriers by examining the effects of two yeast chromatin remodeling complexes, ISW1 and ISW2, on Pol β DNA synthesis in the oligonucleosome templates. Both of these complexes significantly facilitated Pol β DNA synthesis on the folded oligonucleosome arrays *in vitro* (Figure 4). This observation may reflect a need for ATP-dependent chromatin remodeling prior to the Pol β step of BER in chromatin.

Different chromatin structural states may be required for initial and latter steps of BER. Based on our results, we propose a mechanistic model for short-patch BER in chromatin (Figure 5). DNA glycosylases, which are relatively abundant for frequently occurring base damage
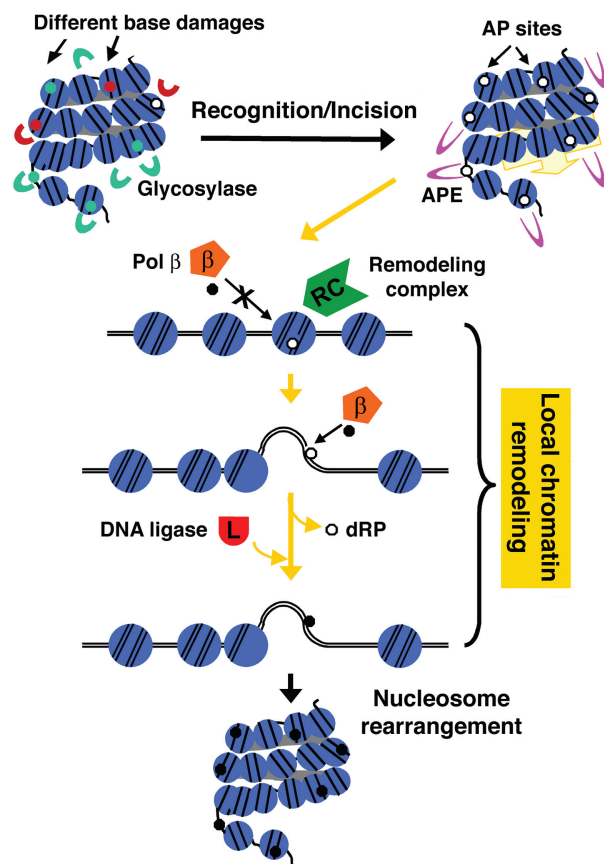
Figure 5. Schematic model of chromatin-remodeling during short-patch BER in chromatin. Damaged bases in chromatin are recognized and incised by a damage-specific DNA glycosylase and abundant APE. Chromatin-remodeling complex then locally disrupts nucleosomes to allow Pol β access to these single nucleotide gaps. Following gap-filling synthesis and removal of dRP group by Pol β, the nick is sealed by DNA ligase, and followed by nucleosome refolding.

(48), continually 'survey' the genome and cleave glycosyl bonds of damaged bases (Figure 5). Subsequently, APE, which is present at high amounts in cells (350 000–700 000 molecules/cell), will incise at AP sites (46,49). Both of these enzymes may act directly on chromatin without requiring significant nucleosome disruption, possibly using the dynamic unwrapping of nucleosome DNA to gain access to internal nucleosome sites. In contrast, Pol β exists at lower levels in cells, ∼50 000 molecules (50), and may only be able to access strand breaks in nucleosome-free DNA, or linker DNA regions. Access of UDG/APE-induced strand breaks within nucleosome core particles, however, may require nucleosome sliding or disruption prior to gap-filling synthesis. After removal of the dRP group by Pol β, the nick is sealed by DNA ligase. Completion of the repair process would then involve rearrangement of the repaired DNA back to the original chromatin structure (Figure 5).

Finally, Chambon and colleagues (51) reported that thymine DNA glycosylase (TDG) associates with transcriptional coactivators CBP and p300. Thus, acetylation of histone tails by the CBP/p300-TDG complex may promote local chromatin relaxation at these sites.

However, relaxation of closed chromatin structure to open form may only be sufficient for Pol β DNA synthesis in linker DNA regions and may not be sufficient for access of Pol β to single-strand breaks in nucleosome core DNA. Indeed, preliminary results do not show a marked promotion of DNA synthesis on oligonucleosomes in the presence of a histone acetyl transferase (HAT1) (Nakanishi and Smerdon, unpublished results). Therefore, complete exposure of nucleosome core DNA, by either nucleosome sliding or disruption may be required to allow Pol β complete access to damaged sites. However, histone acetylation may have important roles in recruitment of additional factors, such as chromatin remodeling complexes, linking these two different chromatin states.

REFERENCES

1. Lindahl,T. and Barnes,D.E. (2000) Repair of endogenous DNA damage. *Cold. Spring. Harb. Symp. Quant. Biol.*, **65**, 127–133.
2. Lindahl,T. (1993) Instability and decay of the primary structure of DNA. *Nature*, **362**, 709–715.
3. Seeberg,E., Eide,L. and Bjoras,M. (1995) The base excision repair pathway. *Trends Biochem. Sci.*, **20**, 391–397.
4. Mol,C.D., Parikh,S.S., Putnam,C.D., Lo,T.P. and Tainer,J.A. (1999) DNA repair mechanisms for the recognition and removal of damaged DNA bases. *Annu. Rev. Biophys. Biomol. Struct.*, **28**, 101–128.
5. McCullough,A.K., Dodson,M.L. and Lloyd,R.S. (1999) Initiation of base excision repair: glycosylase mechanisms and structures. *Annu. Rev. Biochem.*, **68**, 255–285.
6. Mol,C.D., Kuo,C.F., Thayer,M.M., Cunningham,R.P. and Tainer,J.A. (1995) Structure and function of the multifunctional DNA-repair enzyme exonuclease III. *Nature*, **374**, 381–386.
7. Beard,W.A. and Wilson,S.H. (2006) Structure and mechanism of DNA polymerase Beta. *Chem. Rev.*, **106**, 361–382.
8. Duncan,B.K. and Miller,J.H. (1980) Mutagenic deamination of cytosine residues in DNA. *Nature*, **287**, 560–561.
9. Robinson,P.J. and Rhodes,D. (2006) Structure of the '30 nm' chromatin fibre: a key role for the linker histone. *Curr. Opin. Struct. Biol.*, **16**, 336–343.
10. Nilsen,H., Lindahl,T. and Verreault,A. (2002) DNA base excision repair of uracil residues in reconstituted nucleosome core particles. *EMBO J.*, **21**, 5943–5952.
11. Beard,B.C., Wilson,S.H. and Smerdon,M.J. (2003) Suppressed catalytic activity of base excision repair enzymes on rotationally positioned uracil in nucleosomes. *Proc. Natl Acad. Sci. USA*, **100**, 7465–7470.
12. Li,G., Levitus,M., Bustamante,C. and Widom,J. (2005) Rapid spontaneous accessibility of nucleosomal DNA. *Nat. Struct. Mol. Biol.*, **12**, 46–53.
13. Tomschik,M., Zheng,H., van Holde,K., Zlatanova,J. and Leuba,S.H. (2005) Fast, long-range, reversible conformational fluctuations in nucleosomes revealed by single-pair fluorescence resonance energy transfer. *Proc. Natl Acad. Sci. USA*, **102**, 3278–3283.
14. Gowher,H., Stockdale,C.J., Goyal,R., Ferreira,H., Owen-Hughes,T. and Jeltsch,A. (2005) De novo methylation of nucleosomal DNA by the mammalian Dnmt1 and Dnmt3A DNA methyltransferases. *Biochemistry*, **44**, 9899–9904.
15. Bucceri,A., Kapitza,K. and Thoma,F. (2006) Rapid accessibility of nucleosomal DNA in yeast on a second time scale. *EMBO J.*, **25**, 3123–3132.
16. Saha,A., Wittmeyer,J. and Cairns,B.R. (2006) Chromatin remodelling: the industrial revolution of DNA around histones. *Nat. Rev. Mol. Cell. Biol.*, **7**, 437–447.
17. Gaillard,H., Fitzgerald,D.J., Smith,C.L., Peterson,C.L., Richmond,T.J. and Thoma,F. (2003) Chromatin remodeling activities act on UV-damaged nucleosomes and modulate DNA damage accessibility to photolyase. *J. Biol. Chem.*, **278**, 17655–17663.
18. Hara,R. and Sancar,A. (2002) The SWI/SNF chromatin-remodeling factor stimulates repair by human excision nuclease in the mononucleosome core particle. *Mol. Cell Biol.*, **22**, 6779–6787.
19. Ura,K., Araki,M., Saeki,H., Masutani,C., Ito,T., Iwai,S., Mizukoshi,T., Kaneda,Y. and Hanaoka,F. (2001) ATP-dependent chromatin remodeling facilitates nucleotide excision repair of UV-induced DNA lesions in synthetic dinucleosomes. *EMBO J.*, **20**, 2004–2014.
20. Gong,F., Fahy,D. and Smerdon,M.J. (2006) Rad4-Rad23 interaction with SWI/SNF links ATP-dependent chromatin remodeling with nucleotide excision repair. *Nat. Struct. Mol. Biol.*, **13**, 902–907.
21. Hasty,P., Campisi,J., Hoeijmakers,J., van Steeg,H. and Vijg,J. (2003) Aging and genome maintenance: lessons from the mouse? *Science*, **299**, 1355–1359.
22. Izumi,T., Brown,D.B., Naidu,C.V., Bhakat,K.K., Macinnes,M.A., Saito,H., Chen,D.J. and Mitra,S. (2005) Two essential but distinct functions of the mammalian abasic endonuclease. *Proc. Natl Acad. Sci. USA*, **102**, 5739–5743.
23. Hansen,J.C., Ausio,J., Stanik,V.H. and van Holde,K.E. (1989) Homogeneous reconstituted oligonucleosomes, evidence for salt-dependent folding in the absence of histone H1. *Biochemistry*, **28**, 9129–9136.
24. Hansen,J.C., van Holde,K.E. and Lohr,D. (1991) The mechanism of nucleosome assembly onto oligomers of the sea urchin 5 S DNA positioning sequence. *J. Biol. Chem.*, **266**, 4276–4282.
25. Hansen,J.C. and Lohr,D. (1993) Assembly and structural properties of subsaturated chromatin arrays. *J. Biol. Chem.*, **268**, 5840–5848.
26. Van Holde,K. and Weischet,W.O. (1978) Boundary analysis of sedimentation-velocity experiments with monodisperse and paucidisperse solutes. *Biopolymers*, **17**, 1387–1403.
27. Li,S., Waters,R. and Smerdon,M.J. (2000) Low- and high-resolution mapping of DNA damage at specific sites. *Methods*, **22**, 170–179.
28. Dong,F., Hansen,J.C. and van Holde,K.E. (1990) DNA and protein determinants of nucleosome positioning on sea urchin 5S rRNA gene sequences in vitro. *Proc. Natl Acad. Sci. USA*, **87**, 5724–5728.
29. Tse,C. and Hansen,J.C. (1997) Hybrid trypsinized nucleosomal arrays: identification of multiple functional roles of the H2A/H2B and H3/H4 N-termini in chromatin fiber compaction. *Biochemistry*, **36**, 11381–11388.
30. Strobel,S.A. and Cech,T.R. (1995) Minor groove recognition of the conserved G.U pair at the Tetrahymena ribozyme reaction site. *Science*, **267**, 675–679.
31. Schwarz,P.M. and Hansen,J.C. (1994) Formation and stability of higher order chromatin structures. Contributions of the histone octamer. *J. Biol. Chem.*, **269**, 16284–16289.
32. Bellamy,S.R. and Baldwin,G.S. (2001) A kinetic analysis of substrate recognition by uracil-DNA glycosylase from herpes simplex virus type 1. *Nucleic Acids Res.*, **29**, 3857–3863.

33. Tsukiyama,T., Palmer,J., Landel,C.C., Shiloach,J. and Wu,C. (1999) Characterization of the imitation switch subfamily of ATP-dependent chromatin-remodeling factors in Saccharomyces cerevisiae. *Genes Dev.*, **13**, 686–697.

34. Fazzio,T.G. and Tsukiyama,T. (2003) Chromatin remodeling in vivo: evidence for a nucleosome sliding mechanism. *Mol. Cell*, **12**, 1333–1340.

35. Langst,G. and Becker,P.B. (2001) ISWI induces nucleosome sliding on nicked DNA. *Mol. Cell*, **8**, 1085–1092.

36. Flaus,A., Martin,D.M., Barton,G.J. and Owen-Hughes,T. (2006) Identification of multiple distinct Snf2 subfamilies with conserved structural motifs. *Nucleic Acids Res.*, **34**, 2887–2905.

37. Tsukiyama,T., Daniel,C., Tamkun,J. and Wu,C. (1995) ISWI, a member of the SWI2/SNF2 ATPase family, encodes the 140 kDa subunit of the nucleosome remodeling factor. *Cell*, **83**, 1021–1026.

38. Flaus,A. and Owen-Hughes,T. (2004) Mechanisms for ATP-dependent chromatin remodelling: farewell to the tuna-can octamer? *Curr. Opin. Genet. Dev.*, **14**, 165–173.

39. Park,H., Zhang,K., Ren,Y., Nadji,S., Sinha,N., Taylor,J.S. and Kang,C. (2002) Crystal structure of a DNA decamer containing a cis-syn thymine dimer. *Proc. Natl Acad. Sci. USA*, **99**, 15965–15970.

40. Rogakou,E.P., Boon,C., Redon,C. and Bonner,W.M. (1999) Megabase chromatin domains involved in DNA double-strand breaks in vivo. *J. Cell Biol.*, **146**, 905–916.

41. Rogakou,E.P., Pilch,D.R., Orr,A.H., Ivanova,V.S. and Bonner,W.M. (1998) DNA double-stranded breaks induce histone H2AX phosphorylation on serine 139. *J. Biol. Chem.*, **273**, 5858–5868.

42. Paull,T.T., Rogakou,E.P., Yamazaki,V., Kirchgessner,C.U., Gellert,M. and Bonner,W.M. (2000) A critical role for histone H2AX in recruitment of repair factors to nuclear foci after DNA damage. *Curr. Biol.*, **10**, 886–895.

43. Thiriet,C. and Hayes,J.J. (2005) Chromatin in need of a fix: phosphorylation of H2AX connects chromatin to DNA repair. *Mol. Cell*, **18**, 617–622.

44. Fernandez-Capetillo,O., Chen,H.T., Celeste,A., Ward,I., Romanienko,P.J., Morales,J.C., Naka,K., Xia,Z., Camerini-Otero,R.D. *et al.* (2002) DNA damage-induced G2-M checkpoint activation by histone H2AX and 53BP1. *Nat. Cell Biol.*, **4**, 993–997.

45. Slupphaug,G., Mol,C.D., Kavli,B., Arvai,A.S., Krokan,H.E. and Tainer,J.A. (1996) A nucleotide-flipping mechanism from the structure of human uracil-DNA glycosylase bound to DNA. *Nature*, **384**, 87–92.

46. Mol,C.D., Izumi,T., Mitra,S. and Tainer,J.A. (2000) DNA-bound structures and mutants reveal abasic DNA binding by APE1 and DNA repair coordination [corrected]. *Nature*, **403**, 451–456.

47. Sawaya,M.R., Prasad,R., Wilson,S.H., Kraut,J. and Pelletier,H. (1997) Crystal structures of human DNA polymerase beta complexed with gapped and nicked DNA: evidence for an induced fit mechanism. *Biochemistry*, **36**, 11205–11215.

48. Lindahl,T. and Wood,R.D. (1999) Quality control by DNA repair. *Science*, **286**, 1897–1905.

49. Chen,D.S., Herman,T. and Demple,B. (1991) Two distinct human DNA diesterases that hydrolyze 3′-blocking deoxyribose fragments from oxidized DNA. *Nucleic Acids Res.*, **19**, 5907–5914.

50. Horton,J.K., Srivastava,D.K., Zmudzka,B.Z. and Wilson,S.H. (1995) Strategic down-regulation of DNA polymerase beta by antisense RNA sensitizes mammalian cells to specific DNA damaging agents. *Nucleic Acids Res.*, **23**, 3810–3815.

51. Tini,M., Benecke,A., Um,S.J., Torchia,J., Evans,R.M. and Chambon,P. (2002) Association of CBP/p300 acetylase and thymine DNA glycosylase links DNA repair and transcription. *Mol. Cell*, **9**, 265–277.